Sensors and Actuators, 9 (1986) 179 - 197

PROPERTIES OF Ag/AgCl ELECTRODES FABRICATED WITH IC-COMPATIBLE TECHNOLOGIES

L J BOUSSE*, P BERGVELD and H J M GEERAEDTS

Department of Electrical Engineering, Twente University of Technology, P B 217, 7500AE Enschede (The Netherlands)

(Received August 23, 1985, in revised form January 28, 1986, accepted March 10, 1986)

Abstract

The purpose of this work is to fabricate and characterize Ag/AgCl electrodes made on a silicon chip at the wafer level with integrated circuit-compatible fabrication techniques Such electrodes are useful as reference electrodes in several kinds of chemical sensors Two types of electrode were investigated The first type uses an evaporated AgCl layer that is patterned with lift-off photolithography The second type is formed by exposing a selected part of the silver substrate to a $KCrO_3Cl$ solution Both types of electrode give the thermodynamically expected potential response to variations of Cl^- ion concentration The potential generated by the $KCrO_3Cl$-formed electrodes was more stable, however Auger electron spectroscopy depth profiles indicate that immersion in a $KCrO_3Cl$ solution produces a thin layer of AgCl on top of a layer of AgO The low electronic resistance of AgO then reduces the measured series resistance of the $KCrO_3Cl$-formed electrodes Impedance plane plots and the impedance as a function of frequency were measured for both types of electrode, and the impedance of the evaporated AgCl electrodes was indeed considerably higher The impedance measurements could be successfully modelled by assuming a Randles equivalent circuit for the AgCl/electrolyte interface For the $KCrO_3Cl$-formed electrodes, the impedance was modified by the porosity these electrodes manifested

1. Introduction

Work on chemical sensors using integrated circuit fabrication techniques has mainly focused on the development of ion-sensitive field-effect transistors (ISFETs) sensitive to ions such as H^+, Na^+, K^+ and Ca^{++} [1 - 4] Much less attention has been paid to the necessity of incorporating a reference electrode on the sensing chip in order to exploit fully the advantages of

*Present address Stanford Electronics Laboratories, AEL 209A, Stanford University, CA 94305, U S A

0250-6874/86/$3 50

ruggedness and small size for the complete system Harame was the first to incorporate an Ag/AgCl structure on the same chip as an ISFET [5] Recently, Smith and Scott [6] have presented an on-chip Ag/AgCl reference electrode with a reference electrolyte A bare Ag/AgCl electrode is sensitive to Cl^- ions, and is not a generally applicable reference electrode In spite of this, it is clear that the first step towards a batch fabricated on-chip reference electrode will be the deposition of an Ag/AgCl structure on the chip We will concentrate in this paper on the best fabrication technology for such electrodes In various sensing applications, a bare Ag/AgCl electrode is sufficient for the sensor operation, as for example in

(a) The anode in a micromachined Clark cell for the polarographic determination of oxygen [7] A Clark cell on a silicon substrate has been described by Siu and Cobbold [8] and Engels and Kuypers [9]

(b) The reference electrode in a micromachined Severinghaus electrode for the determination of dissolved carbon dioxide Such an electrode is now being developed in our laboratory, based on an ISFET with an added CO_2-permeable membrane

(c) The reference electrode for a differential ISFET/REFET pair, as introduced by Tahara [10] In this case the ISFET is pH-sensitive while the REFET is made pH-insensitive by a polymer coating on the inorganic gate The reference electrode potential is then a common mode signal for the measurement electronics Since it is difficult to obtain a high common mode rejection due to the bad matching of the two transistors, it is desirable to have a stable electrode such as Ag/AgCl rather than the platinum used in ref 10

(d) A quasi-reference electrode for a single ISFET in cases where the Cl^- concentration does not vary significantly, as suggested by Harame [5]

We will report here on the properties of on-chip Ag/AgCl electrodes fabricated with integrated circuit-compatible technologies, *i e*, techniques which form all the electrodes on a whole silicon wafer simultaneously, before the individual chips are scribed, mounted and encapsulated This excludes the usual electrolytic formation of these electrodes, which must be done after encapsulation, although we have made some electrodes of this type for comparison Two wafer-scale fabrication methods were investigated (a) evaporation of silver followed by evaporation of AgCl, (b) evaporation of silver and electroless plating of AgCl using a $KCrO_3Cl$ solution

2 Fabrication procedure

All fabrication was carried out on an oxidized silicon substrate This substrate does not play an active role in the subsequent steps, we have chosen it because of its convenience, and to retain compatibility with integrated circuit chemical sensors such as ISFETs

The first step in device fabrication was the deposition and patterning of a silver layer To obtain adhesion of this layer on the SiO_2 substrate, a thin

primer layer of titanium was used Typical thicknesses were 15 nm of Ti and 400 to 1000 nm of Ag Patterning was done with positive photolithography, the silver being etched with $Fe^{III}(NO_3)_3$ and the titanium with 1 25 HF/H_2O To avoid destroying the silver layer, the resist was stripped with boiling acetone

Next, a permanent protection layer was deposited and patterned The purpose of this protection layer is twofold First, to avoid contact of the silver/titanium sandwich with an electrolyte, which would cause corrosion of the titanium due to the electrolytic cell Ag/electrolyte/Ti, all the edges of the metal sandwich are protected Secondly, the Ag/Ti paths between the bonding pads and the final surface to be chlorided are permanently protected This makes the final epoxy encapsulation of the bond wires during the mounting of the chip less critical, and always leaves an exactly defined electrode surface in contact with the liquid to be measured Figure 1 shows a cross-sectional drawing of the electrodes in this study The area of all types of electrodes was 1 mm^2

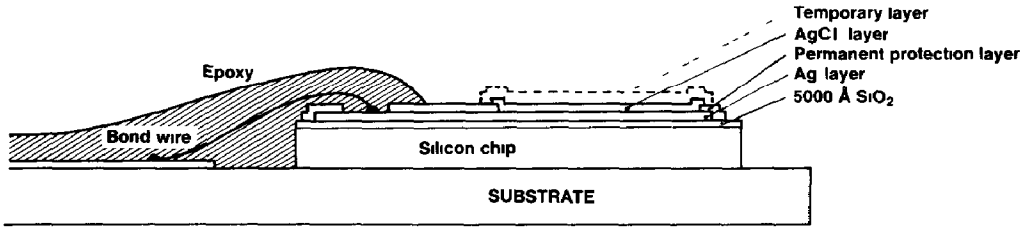

Fig 1 Cross-sectional representation of the Ag/AgCl electrodes fabricated in this work

For most of the samples, the protection layer was Hunt number 3 negative resist, postbaked at 130 °C for 40 minutes A disadvantage of this material, however, was its tendency to swell during the chlorobenzene dip required for the subsequent lift-off (see below) Therefore, we also tried CVD-deposited SiO_2 and polyimide as protection layers Polyimide appears to have the most suitable properties for this application

For the next step, formation of AgCl, two possibilities were tried

(a) First, AgCl was evaporated at a pressure of 10^{-5} Torr Deposition of silver halides in this way has been reported by various authors [11 - 13] Lift-off photolithography was required to pattern the AgCl, and to avoid chemical etching and the possibility of decomposing the AgCl by the u v light involved in photolithography An overhang was created in the Shipley AZ1450J photoresist with a chlorobenzene dip, as reported by Hatzakis *et al* [14] This method of deposing AgCl has the advantage that the silver layer initially present should not be consumed The thickness of the evaporated layer was estimated by weighing, and was typically found to be 200 to 400 nm The lift-off was carried out by dissolving the resist in acetone

(b) The second possibility consisted of dipping the wafer in a 8 g/litre solution of $KCrO_3Cl$ for 2 to 3 minutes [15] This substance was synthesized by the reaction of $K_2Cr_2O_7$ with HCl [16], and further purified by recrystal-

lization Only freshly prepared solutions of $KCrO_3Cl$ were used Photoresist was deposited and patterned to protect those regions of silver that were not to be converted The advantage of this method of chloridizing silver is that the reaction proceeds at a relatively slow rate, which is easy to control Determined by weight increase, we estimate that the silver chloride is formed at a rate of about 100 nm/minute About half the silver layer originally present was transformed, which leads to chloride layers $\approx$200 nm thick

To avoid damaging the AgCl layer by the vapours produced during the curing of the epoxy encapsulant, the AgCl regions were temporarily covered with positive photoresist The last steps of the fabrication procedure consisted of scribing the wafer, mounting the die on ceramic carriers, bonding and encapsulation with epoxy Before testing, the protection layer on the AgCl was removed with acetone

3 Testing procedures

The following measurements were carried out on the encapsulated electrodes

(a) Cell potential measurements were made relative to a standard reference electrode, in particular with respect to the response to Cl^- concentration, stability of the potential and the temperature coefficient Temperature response was measured by slowly varying the temperature of the electrolyte, while the standard reference electrode was kept at room temperature

(b) Complex plane impedance measurements as a function of frequency were carried out using a Schlumberger Solartron 1170 Frequency Response Analyser and a 1186 Electrochemical Interface A standard Ag/AgCl electrode was used as the reference electrode, and a large-area Pt electrode as the counter-electrode The electrolyte was 1M KCl, in a nitrogen or oxygen ambient The evolution of the total impedance with time for some electrodes was measured with a lock-in amplifier All measurements were at room temperature

(c) The structure of the electrodes was inspected in a scanning electron microscope

(d) Auger depth composition profiles were carried out on a Physical Electronics 545A system, with a type 04-191 5 keV rastered ion sputter gun to ensure uniform sputtering

4. Results

4 1 Potential measurements

We measured the potential *versus* Cl^- concentration at 25 °C of a total of 60 electrodes of the evaporated type and of the $KCrO_3Cl$ type, and also including some conventional electrolytically formed electrodes with the

same surface area The sensitivity to Cl^- ions was 56 ± 3 mV per decade of concentration for all electrode types No differences in the potentiometric response to chlorine ions were observed between the two types of electrodes In addition, the temperature dependence of the electrode potential agrees with theoretical expectations, independent of the type of electrode Typical values of dV/dT are shown in Table 1 Concerning stability, however, we observed a marked difference between the evaporated and the $KCrO_3Cl$-formed type of electrode, as shown in Fig 2 Both electrode types show some initial drift, but the long-term stability of the $KCrO_3Cl$-formed electrode is far better

TABLE 1

Measured temperature dependence of the potential of an evaporated AgCl electrode as a function of KCl concentration

Concentration KCl (mol)	Measured dV/dT (mV/°C)	Theoretical dV/dT (mV/°C)
10^{-3}	0 87	—
10^{-2}	0 56	0 61
10^{-1}	0 33	0 43
10^{0}	0 17	0 25
saturated	−0 14	−0 14

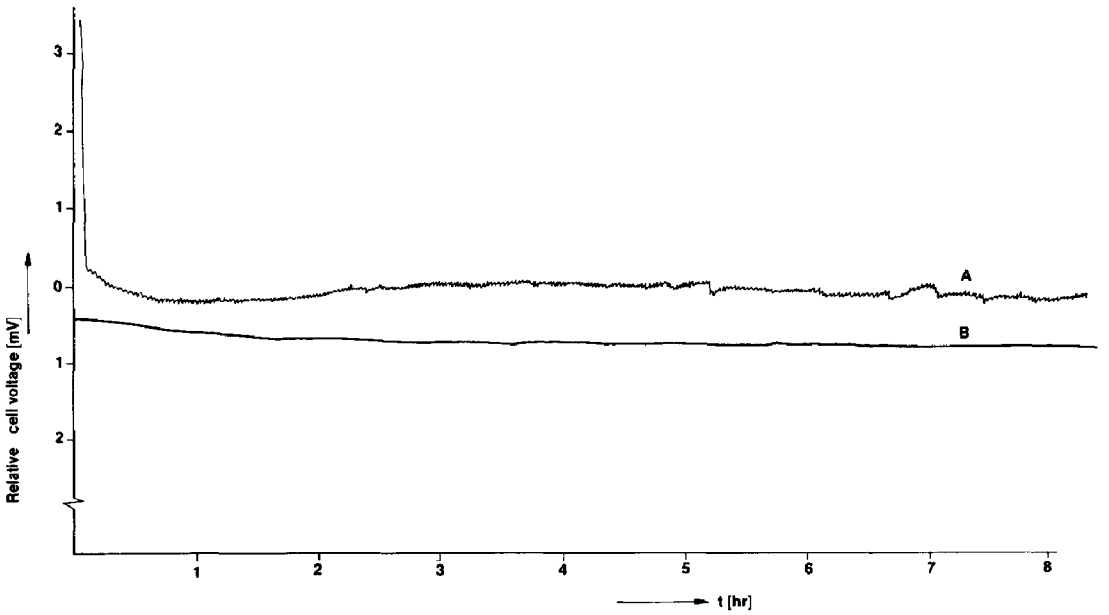

Fig 2 Potential as a function of time after first exposure to the electrolyte (1M KCl + AgCl) of both types of electrode Curve A evaporated AgCl electrode Curve B $KCrO_3Cl$-formed AgCl electrode

4 2 Impedance measurements

Because some time evolution of the impedance of evaporated AgCl electrodes was observed, Fig 3 shows impedance plots after 30 minutes and after six hours at frequencies from 1 Hz to 10 kHz The evolution of the impedance was further studied by measuring the magnitude of the impedance at 200 Hz as a function of time for a number of devices Figure 4 indicates that for evaporated AgCl electrodes stability was achieved after about six hours The general shape of the impedance plot in the complex plane did not change appreciably, the evolution consisted of a reduction of the impedance amplitude at all frequencies Replacing the nitrogen ambient by oxygen produced no significant change in the impedance plot or in the electrode potential, the same was true for the presence or absence of light The impedance plane plot and the impedance as a function of frequency after stability is achieved can be seen in Fig 5 The impedances involved are definitely higher than those obtained with ordinary electrolytic Ag/AgCl electrodes

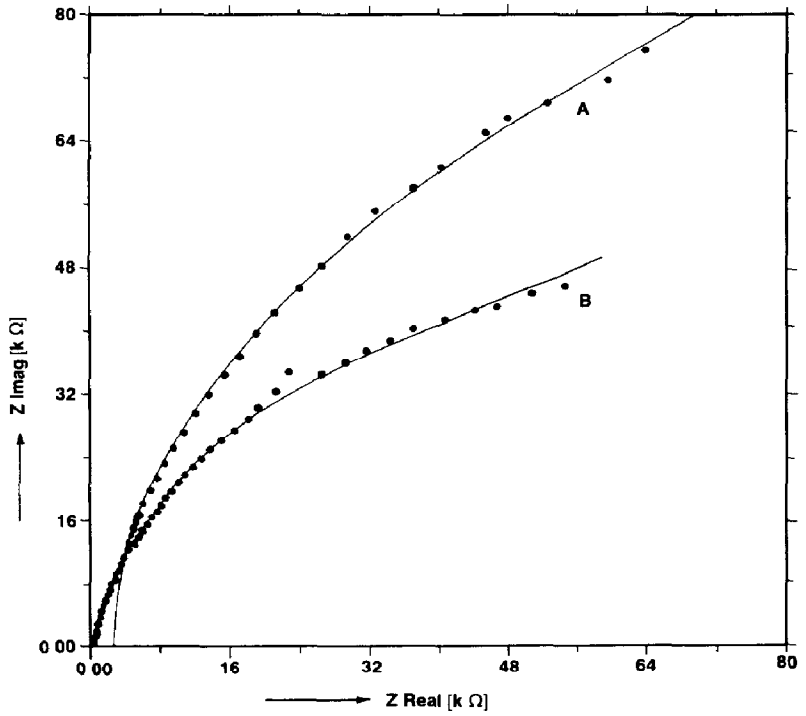

Fig 3 Evolution in time of the impedance plane plot of the evaporated AgCl electrode Curve A after 30 minutes' exposure to 1M KCl Curve B after 6 hours' exposure The solid lines are the theoretical curves calculated with the Randles equivalent circuit of Fig 10 The parameters are, for curve A $C_{DL} = 8\,0 \times 10^{-5}$ F/cm^2, $\theta = 750\ \Omega$ cm^2, $\sigma = 1450\ \Omega$ cm^2 s$^{-1/2}$ and $R_S = 25\ \Omega$ cm^2 For curve B $C_{DL} = 8\,3 \times 10^{-5}$ F/cm^2, $\theta = 460\ \Omega$ cm^2, $\sigma = 830\ \Omega$ cm^2 s$^{-1/2}$ and $R_S = 15\ \Omega$ cm^2

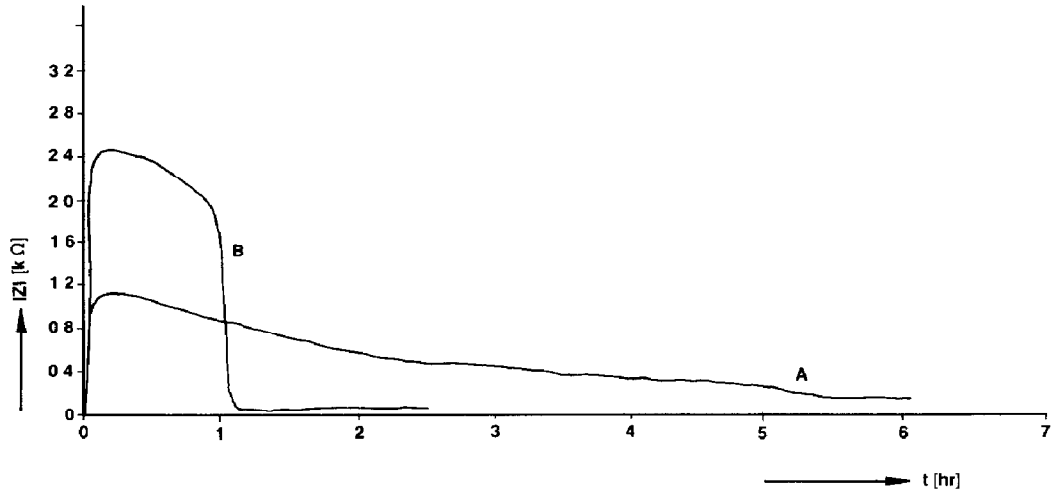

Fig 4 Change of the absolute value of the impedance $|Z|$ at 200 Hz after the first exposure to the electrolyte Curve A evaporated AgCl electrode Curve B $KCrO_3Cl$-formed AgCl electrode

Electrodes made with $KCrO_3Cl$ behaved quite differently The impedance was much lower than for the evaporated types, and drifted considerably more, as shown in Fig 4 This Figure shows a rather abrupt initial change, followed by stable behaviour The impedance plane plot and the impedance as a function of frequency after the initial conditioning are shown in Fig 6 This impedance plane plot looks much like the one expected for Ag/AgCl electrodes, with a Warburg line at low frequencies However, for our electrodes the slope of this line is 20°, which is nearly half the 45° expected Such halving of the phase angle is known to be associated with highly porous electrodes [17]

4 3 SEM pictures

SEM pictures of the surface of both types of electrodes are shown in Figs 7(a) and (b) In both cases, a similar type of granular structure is observed, although for the evaporated AgCl it occurs on a finer scale The rough surface of the $KCrO_3Cl$-fabricated sample suggests that the bulk of the film could also be porous to some extent, in agreement with the phase angle halving observed in Fig 6(a)

4 4 AES depth profiles

An Auger electron spectrum of the surface and a depth profile of an evaporated AgCl electrode are shown in Figs 8(a) and (b) The most remarkable feature of this profile is that nowhere does the AgCl layer seem to have a constant composition Instead there is an almost linear variation of the chlorine signal from the surface to the silver substrate The interface between

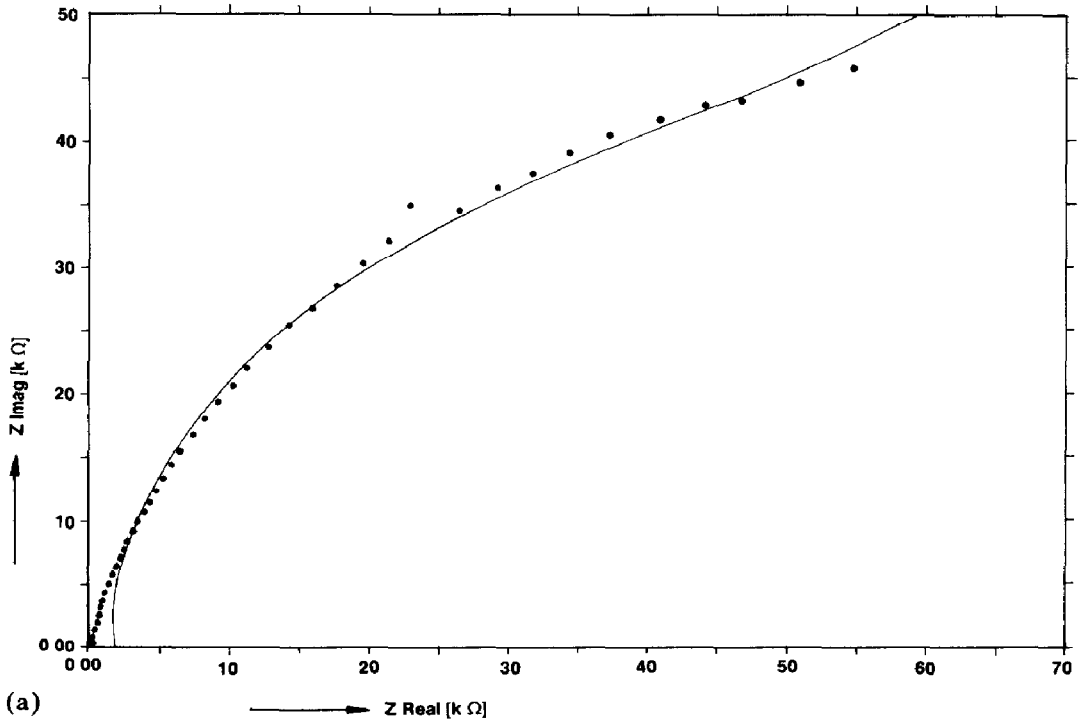

(a)

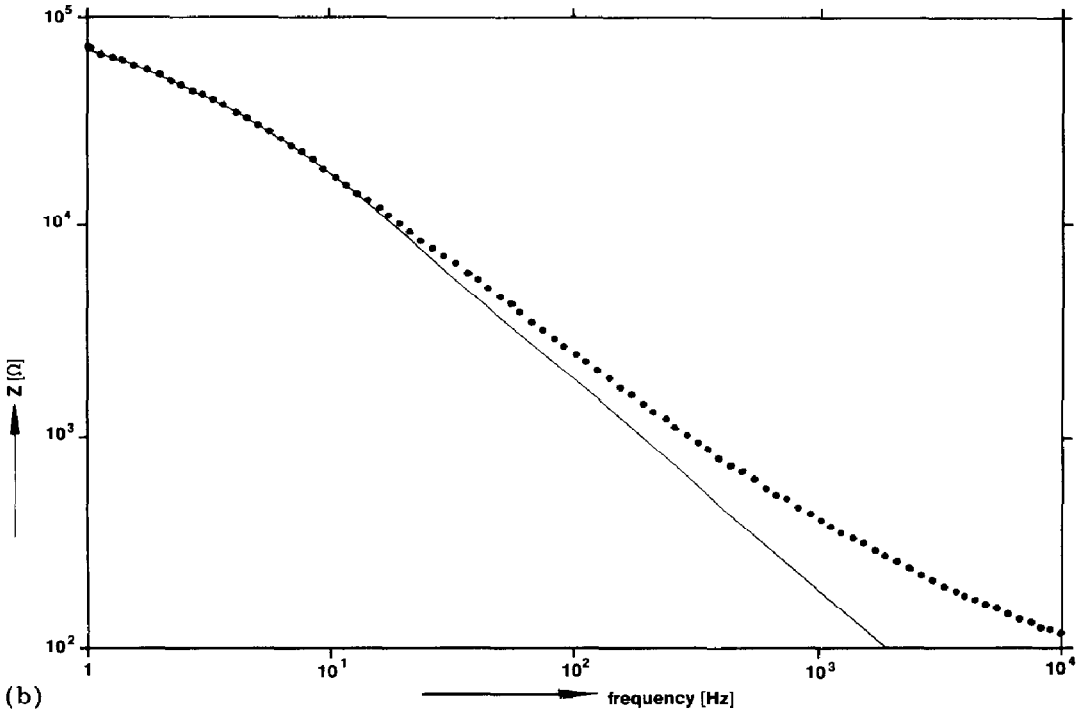

(b)

Fig 5 (a) Impedance plane plot (dots) of the evaporated AgCl electrode after the initial conditioning period (b) Impedance as a function of frequency for the same measurement (dots) The theoretical curves (solid lines) are according to calculations based on the Randles equivalent circuit (Fig 10) and have the same parameter values as curve B in Fig 3

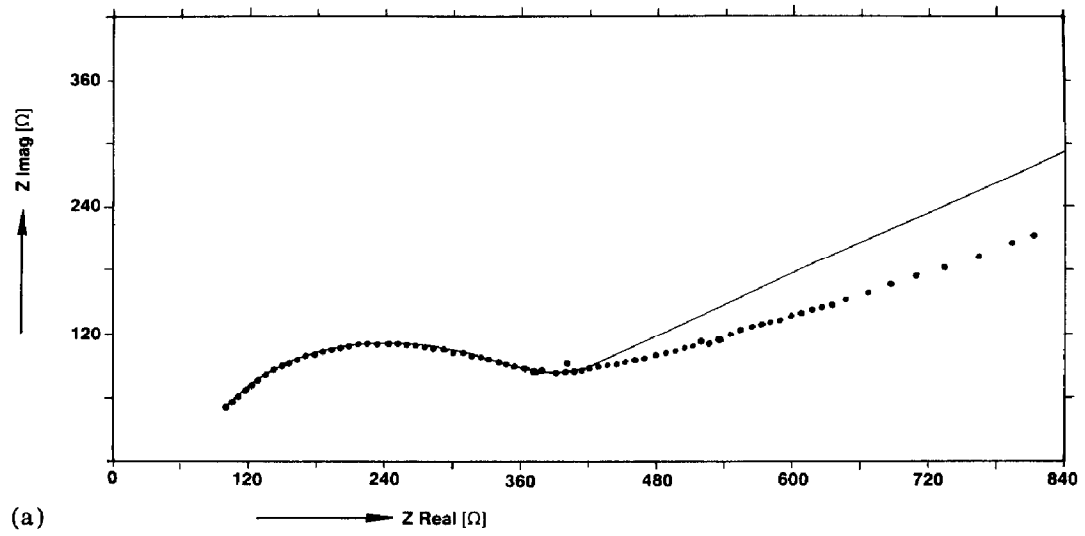

(a)

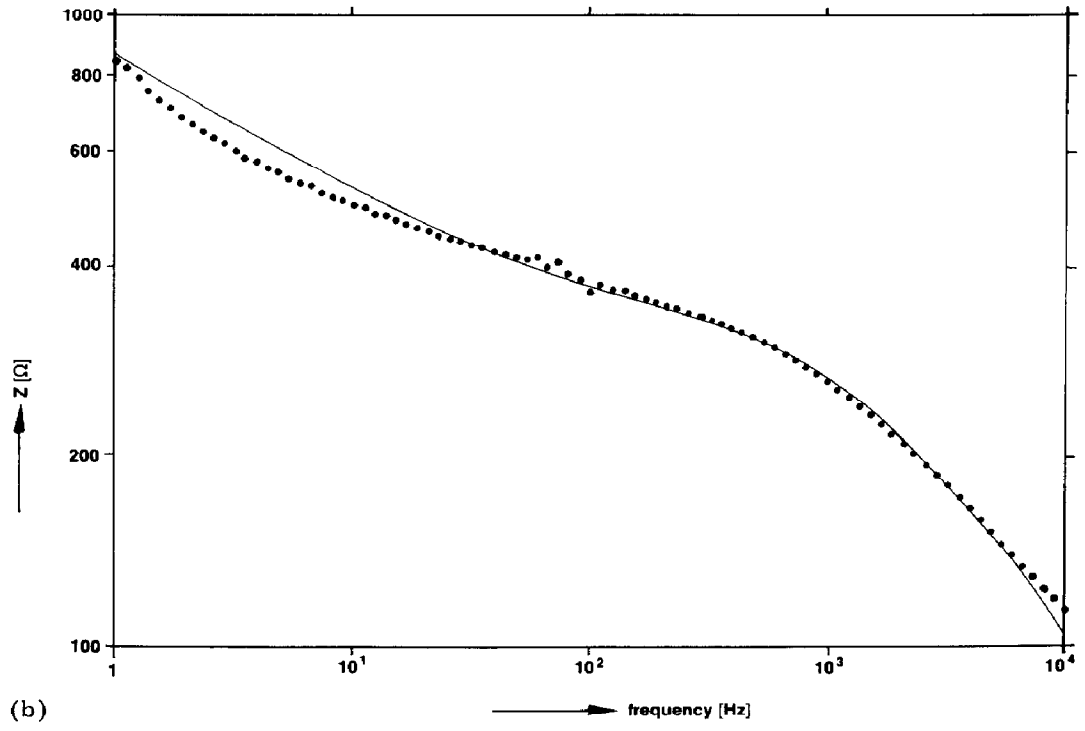

(b)

Fig 6 (a) and (b), same plots as given in Fig 5, but now for a $KCrO_3Cl$-formed AgCl electrode The parameter values for the theoretical curve are discussed in the text

Ag and AgCl is marked by a more rapid change of the chlorine concentration From the surface spectrum and the sensitivity values reported in the AES handbook [18] it follows that the apparent composition at the surface is $AgCl_{0.45}$, a considerable deviation from stoichiometry The same measure-

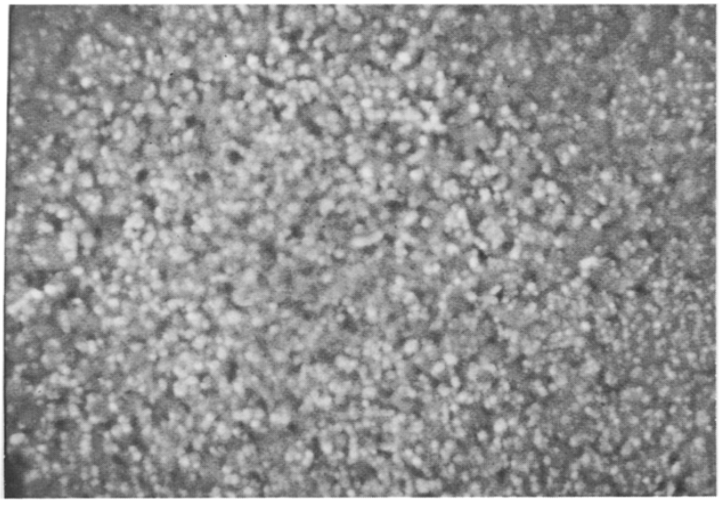

(a)

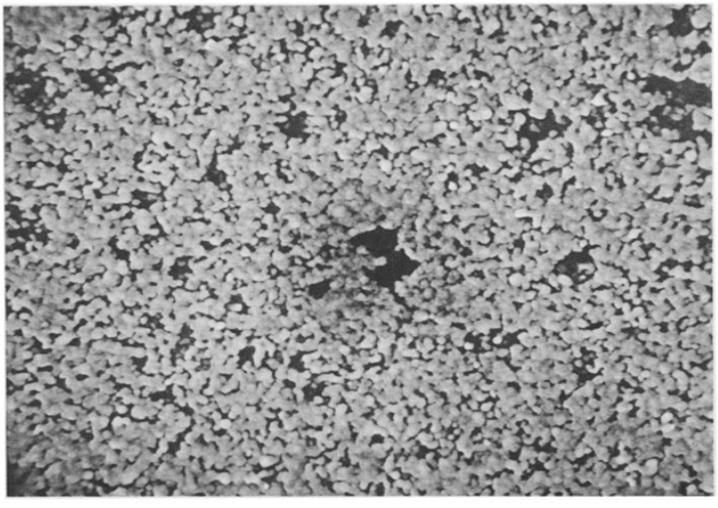

(b)

Fig 7 SEM pictures of the surface texture of the two types of electrodes (a) Evaporated AgCl electrode, magnification 10 500 (b) $KCrO_3Cl$-formed AgCl electrode, magnification 3500

ments on a conventional electrolytically-formed AgCl layer yielded very similar results

Electrodes fabricated with a $KCrO_3Cl$ dip have very different AES depth profiles, as can be seen in Figs 9(a) and (b) Although the surface spectrum shows hardly any oxygen and is very similar to the spectrum for evaporated AgCl shown above, sputtering shows that this oxygen-free surface layer is very thin, and is followed by a layer which is mainly silver

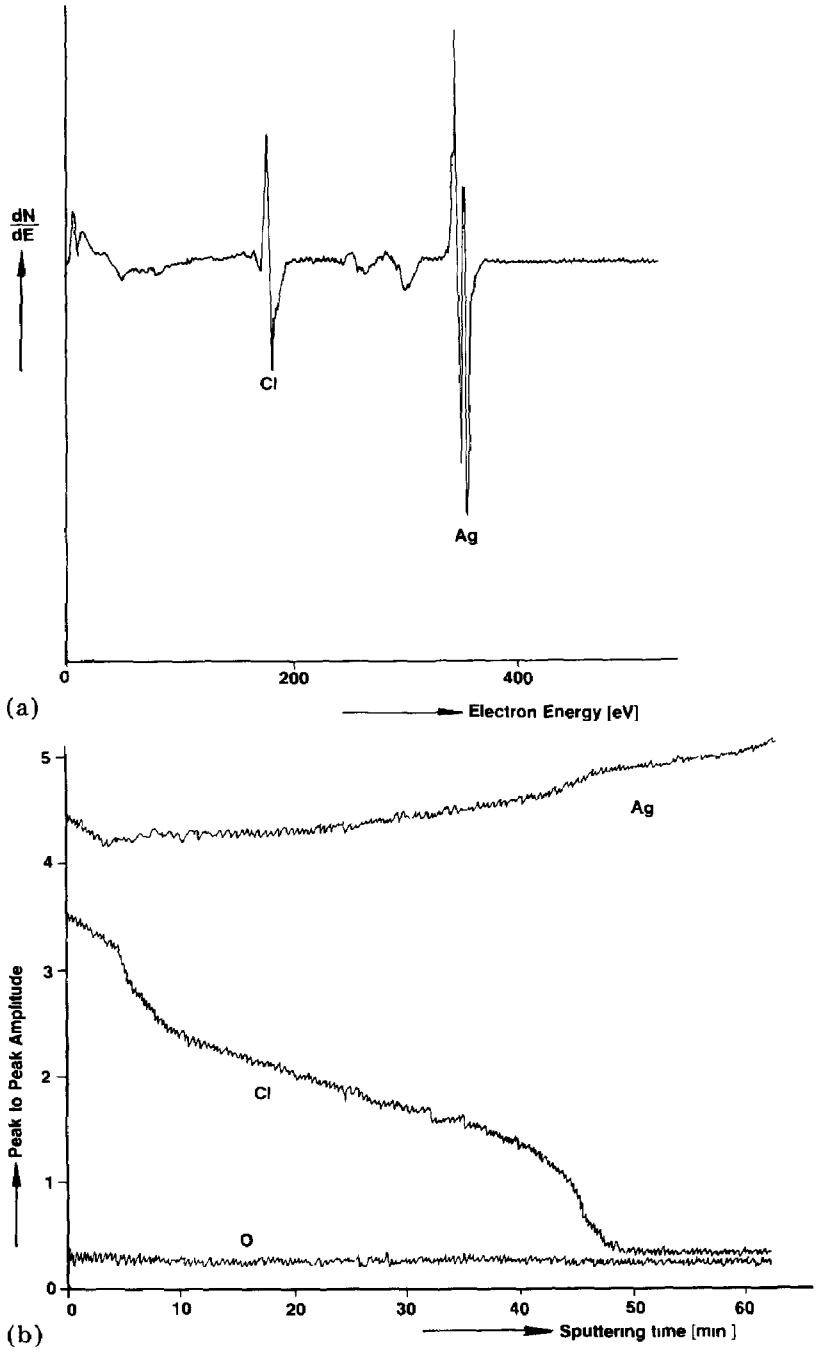

Fig 8 AES analysis of the evaporated AgCl electrode, with a primary electron energy of 3 keV (a) Surface spectrum before sputtering (b) Depth profile obtained by sputtering

oxide Application of the AES handbook [18] sensitivity values gives a layer composition of $AgO_{1\ 05}Cl_{0\ 22}$ Therefore, the silver oxide of this internal layer is similar in composition to the stoichiometric oxide AgO Similar

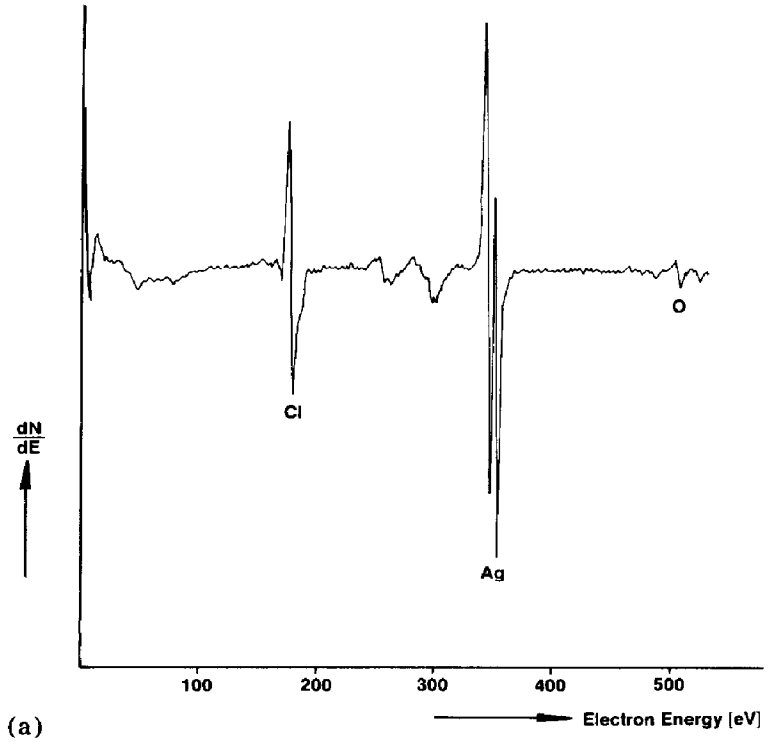

(a)

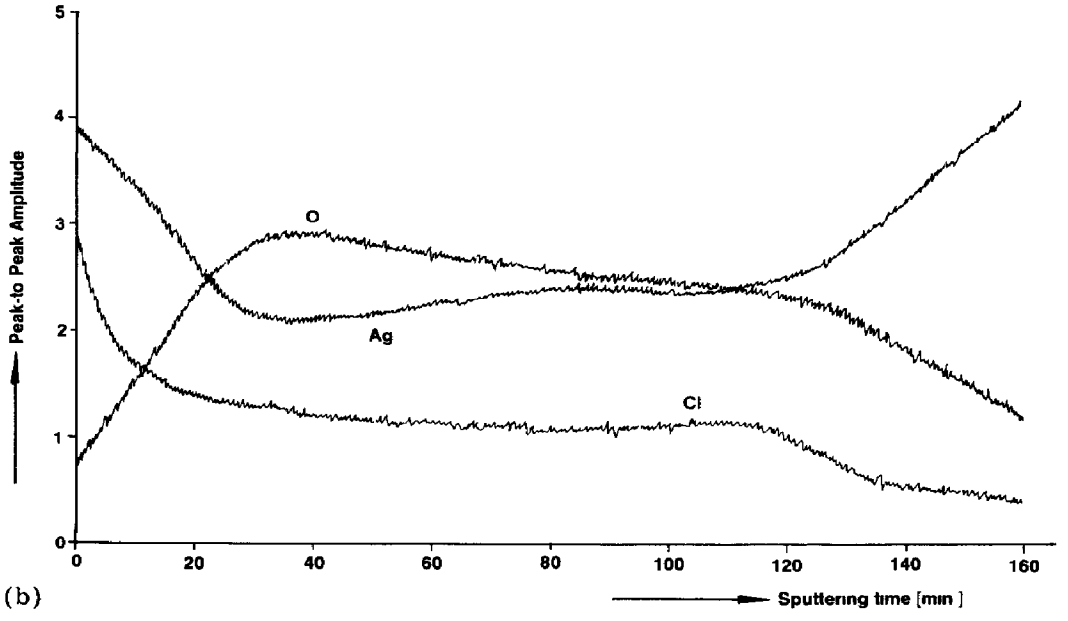

(b)

Fig 9 AES analysis of the $KCrO_3Cl$-formed AgCl electrode, with a primary electron energy of 3 keV (a) Surface spectrum before sputtering (b) Depth profile obtained by sputtering

profiles were found for silver strips immersed in $KCrO_3Cl$ The formation of a thin layer of silver chloride on top of a thicker layer of AgO is therefore typical for the action of $KCrO_3Cl$ on silver

5 Discussion

5 1 Potential measurements

The accuracy and reproducibility of the potential produced by both types of electrodes was similar to that of the classical electrolytic electrodes we produced with the same geometry, and agreed with the thermodynamic prediction We did not apply long aging treatments such as those described in ref 19 for electrolytic electrodes, which improve the accuracy of the potential considerably Longer aging of our electrodes would probably increase the reproducibility of their potential in a similar fashion

5 2 Interpretation of the AES profiles

The structure of the evaporated electrodes is more complicated than would be expected from a simple deposition of stoichiometric AgCl on top of silver The AgCl probably dissociates on evaporation, as indicated by the silver residue we observed in the crucible at the end of the evaporation The volatility of the halogen, leading to some excess silver in evaporated silver halide films, was noted by Baetzold [13] Thus, we expect that the dissociation of silver chloride upon vaporization will produce some chlorine, which will react rapidly with the substrate metal and produce metal chloride Silver halide evaporation should therefore produce films that are similar to those formed by controlled exposure of silver to a halogen, as was done for AgI by Peverelli and van Leeuwen [20] The reaction occurring during evaporation was clearly demonstrated by the experiments of Von Bacho *et al* [12], who evaporated silver halides on various substrate metals They found, for instance, that the surface of an AgBr film evaporated on a copper substrate is richer in copper than in silver, which shows that the mechanism of film formation involves the reaction of the halide with the substrate metal

It would be desirable to obtain more information about the nature of the Ag/AgCl interface in our films through the Auger profiles The problem in the interpretation of these measurements is the tendency of silver halides to dissociate as a result of electron or ion bombardment The chlorine formed by dissociation then desorbs, leaving a surface enriched in silver This effect occurs as a result of the primary electron beam, and explains the lack of stoichiometry as observed in the surface Auger spectra, before any sputtering Very few Auger spectra of silver halide films have been published, Baetzold's results on AgBr films [21] show this artefact even more strongly than ours Benz *et al* [22] have also reported the dissociation of silver halides bombarded with 40 keV electrons, at beam current densities of $1\,6 \times 10^{-5}$ A/cm^2 On alkali halides the electron-induced dissociation and desorption of the halogen have been studied much more extensively [23, 24] The apparent non-stoichiometry we see in our samples can be explained by these effects, and there is no reason to assume that these AgCl surfaces are not stoichiometric In summary, the quantitative interpretation of AES spectra of silver halides is made very difficult by the electron-induced dissociation and desorption which occur Although the evidence in the

literature is less clear about the effect of ion bombardment on the AgCl surface, Baetzold [21] has observed the decrease in the halogen Auger signal as sputtering progresses He attributed the effect to differential sputtering Such a decrease is also evident in the profile of Fig 8(b) It is probable that the decrease in the Cl signal is due to either electron-induced dissociation and desorption, or differential sputtering, or a combination of both

The main value of the AES profiles is to reveal the difference between the two types of electrodes studied here, and in particular to show that the $KCrO_3Cl$-formed electrodes have an intermediate layer, which is a mixture of silver oxide and silver chloride The surface AgCl layer is very thin, of the order of 20% of the total film thickness The composition of the silver oxide is close to AgO, assuming that there is no strong electron-induced dissociation effect in this layer The Auger signals remain relatively constant while sputtering through this layer, which indicates that it is less unstable than AgCl The presence of silver oxide is probably due to the oxidizing action of the chromate ions released by the decomposition of the chlorochromate ions into chlorine and chromate ions

From the previous arguments, it is to be expected that the Cl signal in an AES profile will not correspond to the actual chlorine content, but that the Ag signal will be reliable The presence of a sharp Ag/AgCl interface would therefore manifest itself by a sudden transition in the Ag signal No such sharp transition is observed in any of the electrodes, although it is more marked for the $KCrO_3Cl$-formed electrode, as shown in Fig 9(b) This tends to support the idea that the electrodes fabricated by both methods presented here have no sharp Ag/AgCl interface

5 3 Interpretation of the impedance plots

To interpret the impedance results, a model of the Ag/AgCl electrode is required There is little literature available on the internal structure of the Ag/AgCl electrode, but the Ag/AgI system has been studied in detail by Peverelli and van Leeuwen [25] Their equivalent circuit consists of two interfacial impedances for each of the interfaces, bridged by a geometrical capacitance, which is negligible It is shown in ref 25 that the impedance of the Ag/AgI interface is lower than the impedance of the AgI/electrolyte interface Since there are indications that the Ag/AgCl interface is not sharp anyway, we will neglect the complex part of its impedance and assume that the electrode impedance depends mainly on the AgCl/electrolyte interface This has the further advantage of avoiding complications caused by the complex internal structure of the $KCrO_3Cl$-fabricated electrodes

According to Peverelli and van Leeuwen [20], the impedance of the AgI/electrolyte interface is given by a Randles equivalent circuit (Fig 10) We will assume the same is true for the AgCl/electrolyte interface, implying that the AgCl/electrolyte impedance Z_{EL} is given by the double layer capacitance C_{DL} in parallel with a Faradaic impedance of

$$Z_F = \theta + (1 - j)\sigma\omega^{-1/2} \qquad (1)$$

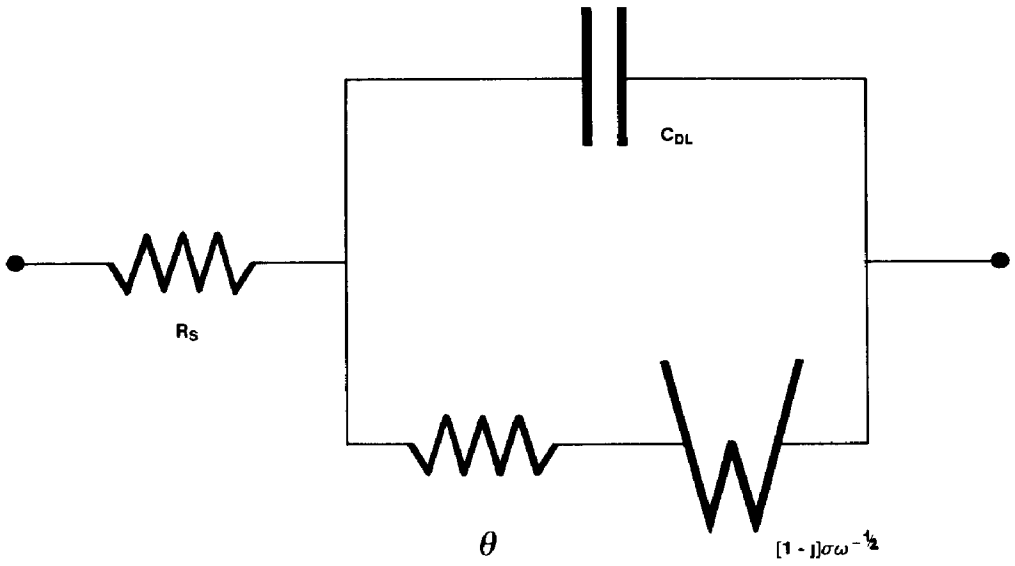

Fig 10 The Randles equivalent circuit used to interpret the impedance behaviour of the electrodes

where σ is the coefficient of the Warburg impedance, and θ is the charge transfer resistance given by

$$\theta = \frac{RT}{Fi_0} \tag{2}$$

and i_0 is the exchange current density of the charge transfer reaction, which is assumed to involve one electron In series with the interfacial impedance is the resistance R_S, which is the sum of the resistance of the electrolyte, the silver substrate, and all internal layers and interfaces Thus, the total measured impedance is given by

$$Z = R_S + Z_{EL} = R_S + \frac{\theta + (1 - j)\sigma\omega^{-1/2}}{1 + j\omega C_{DL}[\theta + (1 - j)\sigma\omega^{-1/2}]} \tag{3}$$

The equivalent circuit of Fig 10 will first be used to interpret the impedance measurements obtained with the evaporated Ag/AgCl electrode The theoretical complex impedance plane plot, and the impedance *versus* frequency plot obtained from the equivalent circuit, can be found in Figs 5(a) and (b), together with the experimental data The agreement with measurement is very good in the low-frequency region, up to about 100 Hz At higher frequencies, the experimental curve approaches the real axis at an angle of 65° instead of the 90° expected on the basis of the Randles equivalent circuit This reduction of phase angle could be due to the porosity or roughness of the electrode, which is visible on Fig 7(a), beginning to manifest itself at those frequencies The values of C_{DL}, θ and σ were obtained as follows In the complex impedance plane plot, θ follows directly from the curvature of the circular part of the plot The point at which the

Warburg impedance starts to affect the curve depends on $\theta^2 C_{DL}$, which is determined by fitting the experimental curve Finally, fitting the theoretical plot of $|Z|$ *versus* frequency to the experimental results yields the individual values of θ and C_{DL} The values found in the 1M KCl solution were $C_{DL} = 8\,3 \times 10^{-5}$ F/cm^2, $\theta = 460\ \Omega\ \text{cm}^2$, and $\sigma = 830\ \Omega\ \text{cm}^2\ \text{s}^{-1/2}$ We have not applied any correction to these values to take account of the difference between real and apparent surface area, which should be borne in mind when comparing our results to those in ref 25, where a correction factor of 1 5 is applied

The series resistance times unit area R_S is found to be about 15 Ω cm^2, and is probably mostly due to the high electronic resistance of the AgCl layer The bulk resistivity of thin evaporated AgCl films has been measured by Baetzold [13], for the (111) orientation at room temperature his result is $10^7\ \Omega$ cm A similar value for amorphous thin films is cited by Janz [19] Since the thickness of our evaporated AgCl films is of the order of 300 nm, a series resistance of 300 Ω cm^2 would be expected In fact, the observed resistance is more than an order of magnitude smaller This phenomenon is well known for electrolytic AgCl electrodes, where a discrepancy of a factor of 10 to 100 is seen [19] Various explanations for this, including porosity, have been advanced Another possibility is that the AgCl layers involved here have sufficient silver to increase their conductivity appreciably

The impedance plane plot of the $KCrO_3Cl$-formed electrode is quite different, and it can be seen that the phase angle is approximately halved compared to the previous electrodes This suggests the presence of porosity According to de Levie [17], the impedance of an electrode with sufficiently long and narrow pores is given by

$$Z_P = a\sqrt{Z_{EL}} \tag{4}$$

The proportionality constant a depends on the pore size distribution and on the resistivity of the electrolyte solution, and Z_{EL} is the impedance per unit of true area of the AgCl/electrolyte interface This expression assumes pores that are much narrower than they are deep Since the thickness of the AgCl layer for these electrodes is only about 200 nm, the pores must have dimensions smaller than 20 nm As before, the total measured impedance is given by

$$Z = Z_P + R_S \tag{5}$$

Figures 6(a) and (b) show how theoretical curves generated by eqns (4) and (5) fit the experimental data The fit is excellent for the semicircular region of the impedance plane, but the slope of the Warburg line is somewhat less than the 22 5° expected from the theory for a perfectly porous electrode It is therefore clear that at low frequencies this theory does not entirely apply The theoretical parameters are determined by the same procedure as described above, with one difference with the addition of the extra parameter

a there is redundancy in the parameter set, and values of θ, σ, and C_{DL} can be determined for each a If one chooses to force the double layer capacitance to be the same as for the evaporated AgCl electrode, then the other parameters for a 1M KCl solution are $\theta = 1\ 47\ \Omega\ cm^2$, and $\sigma = 20\ 5\ \Omega\ cm^2\ s^{-1/2}$ These values do not have much absolute meaning, but they do indicate that relative to the double layer capacitance, the charge transfer resistance is much lower in this case A possible explanation for this is the presence of surface texture on a much finer scale than can be imaged with a SEM As Peverelli and van Leeuwen have argued [20], if there is surface roughness on a scale smaller than the double layer dimensions, then the double layer capacitance does not change but the effective area for the charge transfer reaction increases This again suggests the presence of roughness or pores on a distance scale of the order of nanometers

The series resistance in this case is about $0\ 045\ \Omega\ cm^2$, which is much lower than for the evaporated electrodes This can be explained by assuming that the internal layer is indeed mainly AgO, as the Auger profile indicates, since AgO is a good electronic conductor

The initial evolution of the impedance is another indication of the porosity of the $KCrO_3Cl$-formed electrodes The considerable decrease of the impedance during the first hour of exposure to an electrolyte shows an increase of surface area This can be interpreted as a filling of the small pores present after the $KCrO_3Cl$ treatment

6. Conclusions

We have demonstrated that both methods of electrode fabrication yield electrodes with the expected potential in chloride solutions However, it is also clear that the $KCrO_3Cl$-formed electrodes have the following advantages

(a) The electrode potential is more stable and reaches stability faster, making more precise measurements possible

(b) Low series impedance due to the highly conductive AgO layer, and low total impedance due to a high effective surface area

(c) Ease of fabrication, all that is required is a dip of the encapsulated electrode in the $KCrO_3Cl$ solution

These advantages mean that the $KCrO_3Cl$-fabricated electrodes are the most suitable candidates for the applications listed above A possible disadvantage is the thinness of the AgCl layer of these electrodes, which might make them more vulnerable to the electrolytic dissociation of the AgCl layer due to the passage of current

The understanding of the internal functioning of all these Ag/AgCl electrodes is still incomplete We have found that a first order approach to understanding the electrode impedance yields reasonably good results, but the explanation is not perfect Especially for the $KCrO_3Cl$-fabricated electrodes, the internal structure is complex, and it would be difficult to take

account of it in a satisfactory way More impedance measurements in a wider range of conditions would be required to elucidate these points

Acknowledgements

The authors thank Prof J Vereecken and O Steenhaut of the Electrochemistry Laboratory of the Vrije Universiteit Brussel for putting their facilities for Auger measurements and impedance plane measurements at our disposal Dr R Vounckx assisted in collecting some of the experimental data One of the authors (L B) thanks the Nationaal Fonds voor Wetenschappelijk Onderzoek (Belgium) for providing him with a fellowship

References

1 P Bergveld, *IEEE Trans Biomedical Eng , BME-19* (1972) 342
2 J Janata and R J Huber, in H Freiser (ed), *Ion-Selective Electrodes in Analytical Chemistry*, Vol 2, Plenum, New York, 1980, p 107
3 H Abe, M Esashi and T Matsuo, *IEEE Trans Electron Devices, ED-26* (1979) 1939
4 L Bousse, N F De Rooij and P Bergveld, *IEEE Trans Electron Devices, ED-30* (1983) 1263
5 D Harame, J Shott, J Plummer and J Meindl, *Digest of the 1981 Int Electron Devices Meet* , p 467
6 R L Smith and D C Scott, *Proc IEEE/NSF Symp on Biosensors, Los Angeles, Sept , 1984*, p 61 (IEEE 84CH2068-5)
7 I Fatt, *Polarographic Oxygen Sensors*, CRC Press, Boca Raton, FL, 1976
8 W M Siu and R S C Cobbold, *Med Biol Eng Comp , 14* (1976) 109
9 J M L Engels and M H Kuypers, *J Phys E, 16* (1983) 987
10 S Tahara, M Yoshii and S Oka, *Chem Lett* , (1982) 307
11 R P Buck and D E Hackleman, *Anal Chem , 49* (1977) 2315
12 P S Von Bacho, G P Caesar, H M Saltsburg and R C Baetzold, *J Vac Sci Technol , 13* (1976) 107
13 R C Baetzold, *J Phys Chem Solids, 35* (1974) 89
14 M Hatzakis, B J Canavello and J M Shaw, *IBM J Res Develop , 24* (1980) 452
15 16113 Ion Selective Electrode, example 2, *Res Disclosure*, Sept 1977, p 35
16 G Brauer, *Handbuch der preparativen anorganischen Chemie*, Enke Verlag, Stuttgart, 2nd edn , 1962, p 1215
17 R De Levie, *Electrochim Acta, 10* (1964) 1231
18 P W Palmberg, G E Riach, R E Weber and N C MacDonald, *Handbook of Auger Electron Spectroscopy*, Physical Electronics, 1972
19 G J Janz, Silver–silver halide electrodes, in D J G Janz and G J Ives (eds), *Reference Electrodes, Theory and Practice*, Academic Press, New York, 1961, p 179
20 K J Peverelli and H P van Leeuwen, *J Electroanal Chem Interfacial Electrochem , 99* (1979) 157
21 R C Baetzold, *Appl Phys Lett , 26* (1975) 709
22 V Benz, R Ostwald and K G Weil, *Ber Bunsenges Phys Chem , 80* (1976) 1168
23 H Tokutaka, M Prutton, I G Higginbotham and T E Gallon, *Surface Sci , 21* (1970) 233
24 A Friedenberg and Y Shapira, *Surface Sci , 87* (1979) 581
25 K J Peverelli and H P van Leeuwen, *J Electroanal Chem Interfacial Electrochem , 110* (1980) 119

Biographies

Piet Bergveld was born in Oosterwolde, the Netherlands, on January 26, 1940 He recieved the M S degree in electrical engineering (electronics) from Eindhoven University of Technology, Eindhoven, the Netherlands, in 1965, and the Ph D degree from Twente University of Technology, Enschede, the Netherlands, in 1973

Since 1965 he has been a member of the Bio-information Group, Department of Electrical Engineering, Twente University of Technology He is further a member of the Coordination Centre for Biomedical Engineering and a member of the Research Unit Sensors and Actuators of this University In 1981 he became a member of the Semiconductor Group of the Foundation for Fundamental Research on Matter in the Netherlands

The subject of his dissertation was the ion-sensitive field-effect transistor (ISFET) and the OSFET He is involved in research on electronic measuring and stimulating methods in physiological systems with special attention on *in vivo* biosensors He lectures on biomedical instrumentation for graduate students of Twente University of Technology and medical personel of affiliated hospitals

In 1984 he was appointed as full professor in biosensor technology at the Twente University of Technology

Luc Bousse was born in Brussels, Belgium in 1955 He studied engineering at the Vrije Universiteit Brussel, where he obtained the Electrical Engineer's degree in July 1977 That same year he obtained a fellowship from the Belgian Foundation for Scientific Research In Brussels University, he started work on silicon sensors, which was continued in 1979 in the Bio-information Group in the Department of Electrical Engineering of the Twente University of Technology, Enschede, The Netherlands There he obtained a Ph D degree in 1982, with a thesis on the theory of electrolyte/insulator/silicon structures In 1983 he joined the Electrical Engineering Department of Stanford University, Stanford, California, where he is now a research associate His research interests are chemical sensors and silicon technology

Harry Geeraedts was born in Kerkrade, the Netherlands in 1958 He studied chemical engineering at the Institute of Technology in Heerlen, where he obtained his degree in 1981 He worked on ISFETs in the Biosensor group at the Twente University of Technology from 1981 to February 1984 He then became technical assistant in the laboratory for Sensors and Actuators at the same University In September 1985 he moved to Matra GCA in Nantes, France, as process engineer for microlithography, resist processing and dry-etching